Available online www.jocpr.com

Journal of Chemical and Pharmaceutical Research, 2014, 6(3):735-744

Research Article

ISSN : 0975-7384
CODEN(USA) : JCPRC5

A simplified mechanistic model for predicting the critical incipient velocity of cuttings in inclined pipes

Haolin Zhang, Gensheng Li, Shouceng Tian and Xianzhi Song

State Key Laboratory of Petroleum Resources and Prospecting, China University of Petroleum, Beijing, PR China

---

ABSTRACT

By the analysis of cuttings transport mechanism, a simplified mechanistic model for predicting the critical incipient velocity of cuttings in the inclined pipe was presented in this paper based on the balance of force and moment. Drag coefficient calculation method was introduced into the model to improve the prediction accuracy. The incipient movement of different cuttings at certain angle was observed under different flow rate of water and glycerol solution. The numerical results of present model are in good agreement with experimental data and both of which indicate the domination of suspension transport mechanism at low inclination angle, and the domination of rolling transport mechanism in the range of medium angle to horizontal. By the analysis of rolling transport velocity and suspension transport velocity of the particle in X-Y axis, both of which are calculated by the model, we can get the change law of critical incipient velocity of cuttings in inclined pipes. In particular, the maximum critical incipient velocity of cuttings was reached at about 60°of inclination while the minimum value is reached at lower inclination angle. The position of minimum value was determined by drag coefficient, lift coefficient and inclination angle.

Key words: Solid-liquid flow; cuttings transport; transport mechanism; mechanistic model; critical incipient velocity;

INTRODUCTION

Resuspension or remigration of particles from bed surface over which fluid flows is frequently encountered in many industrial processes, such as chemical engineering, metallurgy leaching and flotation, deep-sea mining, hydraulic coal mining, petroleum drilling and river sludge removing etc. Especially in petroleum drilling, deposition of cuttings on the low side of wellbore will induce a series of drilling problems even drilling accidents. Determining the flow conditions under which particles will detach and move from bed surface is a difficult task and central to this task are impending motion models, which are typically created by considering force and moment balances on a particle based on particle transport mechanism [1,2] . According to this theory, some researchers [3-5] have established several critical velocity models. However, these models are either too complex or inadequately accurate to apply in engineering.

In the present study, we analyzed particle transport mechanism in inclined pipes. According to the mechanism, a simplified mechanistic model of critical incipient velocity for particle movement was proposed. As a first step, the micro forces such as plastic force, pressure force, added mass force and Basset force are neglected to simplify particle force analysis. Then the drag coefficient and the lift coefficient were optimized separately to improve the calculation accuracy of the model. Finally, particle transportation experiments were carried out to validate the simplified mechanistic model and the main results were summarized.

CUTTINGS TRANSPORT MECHANISMS

In vertical and nearly vertical pipe (inclination angle less than 10°), cuttings tend to sink along the pipeline axial due to gravity effect. However, the relative velocity between fluid and cuttings generates a drag force on particle. The drag force increases with the settling velocity and finally equals to gravity. At this point, the cuttings velocity comes to a constant which is defined as the terminal setting velocity. As the settling direction of cuttings is contrary to that of fluid velocity in the same line, cuttings will be slowly carried out of wellbore by fluid as long as the upward velocity of fluid is slightly greater than terminal settling velocity of cuttings and ensure the continuous circulation of fluid. Therefore, there is no sedimentary bed in vertical section and cuttings transport mechanism is suspension transport, as shown in Fig.1.

In the inclined pipe, cuttings always suffer axial component and radial component of the gravitational force. It tends to deposit along the axial direction to the bottom under the effect of axial component of the gravitational force. However, cuttings tend to deposit on low side of pipeline under the effect of radial component of the gravitational force. If the fluid velocity is large enough, the fluid force acting on a particle overcomes its gravity, suspends and transports the particle. The cuttings will be in suspension transport state right now, as shown in Fig.2a. Some cuttings may deposit and stagnate on the low side of tube wall to form a sand bed, the reasons are radial component of the gravitational force of particle reaches a certain value in the condition of the large inclination angle and the fluid force acting on the particle diminishes as the fluid flow rate steadily decreases. Under this condition, cuttings on the top of sedimentary bed are in rolling transport; however, cuttings at the bottom of sedimentary bed are in standstill state, as shown in Fig. 2b. More cuttings will deposit as further reduction of the fluid flow rate and the thickness of sedimentary bed gradually increases. The axial component of the gravitational force of particle reaches a critical value to slide downward until the bed thickness accumulates to a certain extent. Therefore, the bottom of bed will avalanche downward along the pipeline. In this situation, the bottom of sedimentary bed is in avalanche downward state while the cuttings on bed surface are in rolling transport state because of the action of fluid flow, as shown in Fig. 2c.

In horizontal pipe, the direction of cuttings gravity-sedimentation is perpendicular to that of fluid flow and the resultant velocity deviates from the axis of pipe to its low side. For this reason, cuttings are likely to deposit and initiate sedimentary bed at the lower side of pipe. As shown in Fig. 3a, cuttings on surface of sedimentary bed begin to slide with fluid velocity gradually increasing. Due to bumpy surface of the sedimentary bed, cuttings mainly transport through tumbling and saltation. However, cuttings below the surface remain stationary in the original position. The drag force of fluid not only can act on surface particles of sedimentary bed, but also act on particles below the surface. When fluid velocity reaches a certain value, some cuttings below the surface begin to move because of the increase of drag force and momentum exchange between each layer of cuttings. As the liquid flow continuously enhanced, the movement of cuttings gradually develop to the deep of sedimentary bed and finally generate a layer movement of cuttings. When a large number of cuttings transport in the form of moving bed, it can be assumed that there is no mass exchange between adjacent layers in macroscopic view, as shown in Fig. 3b. When the fluid velocity is large enough, movement exchange and mass exchange occur simultaneously between adjacent layers of cuttings account for the diffusion of turbulence. Cuttings get into suspension transport state with the influence of lift force and radial pulsations of fluid, as shown in Fig. 3c.

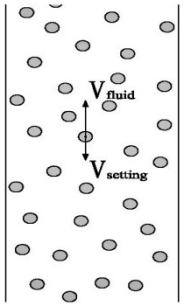

Fig.1 Suspension transport in vertical pipe

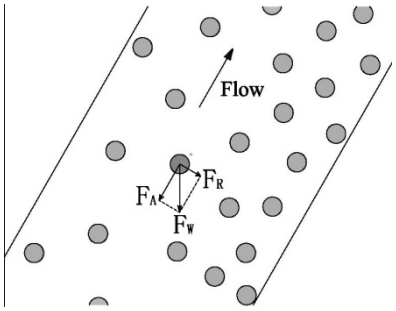

Fig.2a Suspension transport in inclined pipe

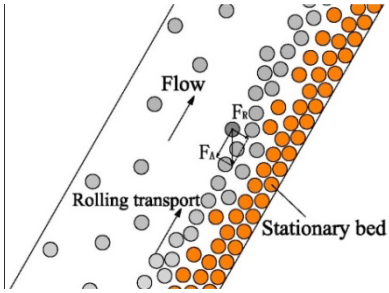

Fig.2b Rolling transport in inclined pipe

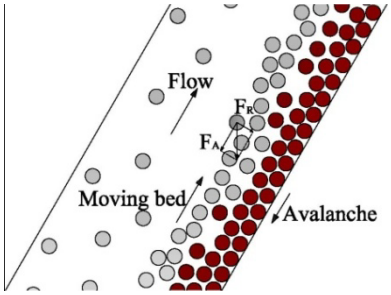

Fig.2c Moving bed transport and avalanche in inclined pipe

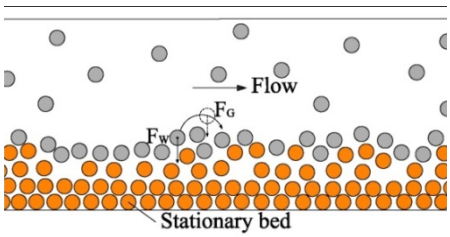

Fig.3a Rolling transport in horizontal pipe

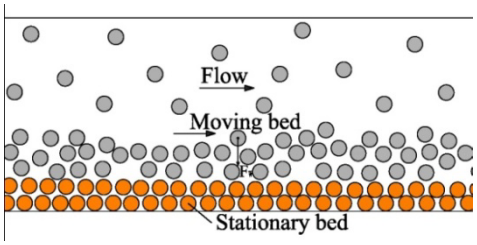

Fig.3b Moving bed transport in horizontal pipe

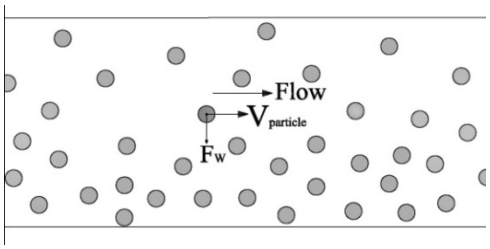

Fig.3c Suspension transport in horizontal pipe

MODEL DEVELOPMENT

Mathematical modeling of cuttings transport phenomena in pipes is quietly complicate and requires considerable idealizations of the hydrodynamics in the fluid flow and the characters of the cuttings.

1) The fluid in steady state and fully development flow is isothermal and time-independent without end efforts.
2) The cuttings can be represented by spherical particles with uniform size, density and friction angle.
3) The sedimentary bed on the lower side of pipe has a uniform thickness and uniform arrangement.
4) The cuttings do not affect the fluid velocity and viscosity.
5) To simplify particle force analysis by considering the main forces such as net weight, drag force and lift force and neglecting the micro forces such as plastic force, pressure gradient force, added mass force and Basset force.

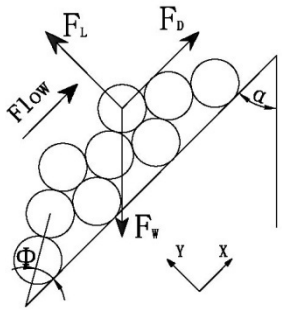

Fig.4 Cuttings arrangement of sedimentary bed and the main forces acting on a surface particle in an inclined pipe

Assuming there is a sedimentary bed with a uniform arrangement on the lower side of pipe as shown in Fig. 4 and the angle of repose of cuttings is assumed to be 30°. The interaction between cuttings and fluid is realized through momentum exchange, and the key points to analyze the motion state of single particle are the determination of the forces acting on the particle and force and moment balances on it. When the hydrodynamic forces exerted by fluid

flowing over a particle on sedimentary bed surface exceed its static forces, the particle begins moving. Therefore, forces acting on a particle should be studied firstly before the determination of its motion state.

There are gravitational force and buoyancy force acting on the cuttings that sediment in fluid and the difference between the two forces is called buoyant weight.

$$F_W = \pi d_p^3 (\rho_p - \rho_f) g / 6 \tag{1}$$

When there is relative movement between the cuttings and its surrounding fluid, it will experience a drag force in the same direction of fluid. The drag force is the result of pressure and shear stress acting on the cuttings surface and theoretically it can be calculated with integration method, however, the ideal mathematical method is difficult to application as it is hard to determine pressure and shear stress distribution across the particle surface. As a result, other convenient methods are applied in theoretical calculation.

Tsuji [6] has presented a correlation that can be used to estimate the drag force acting on bed cuttings:

$$F_D = C_D \pi d_p^2 \rho_f u^2 / 8 - \pi d_p^3 dp / (6dx) + f_D \tag{2}$$

The first term on the right side of equation (2) is the steady part of drag force, the second is pressure gradient term and the third is the unsteady part of drag force. The unsteady part of drag force f_D includes the added mass force and Basset force exerted by the diffusion of vortexes generated on cuttings surface into the surrounding fluid. However, Caulet[7] and Meng[8] found that both the second and third terms can be neglected in low-pressure gradient and steady uniform flow. Therefore, the drag force equation applied in this paper can be expressed as:

$$F_D = C_D \pi d_p^2 \rho_f u^2 / 8 \tag{3}$$

The cuttings will experience the drag force in all types of flow states when fluid flowing over a sedimentary bed. Usually, the drag force is superior over all other forces and affects cuttings transportation. From equation (3) we can see that the key point to calculate drag force is to determine the drag coefficient C_D. The drag coefficient is a function of shape, size, roughness and orientation of non-spherical particles, fluid properties and flow parameters. Usually, particle Reynolds number Re_p is used to estimate the drag coefficient C_D for rigid spherical particles. The particle Reynolds number Re_p is defined as

$$\mathrm{Re}_p = \rho_f u d_p / \mu \tag{4}$$

Because the flow states during flow process are quietly complicated, the drag coefficient cannot be expressed an analytical form for a wide range of particle Reynolds numbers. Some researchers [9,10] determined the drag coefficient values of single particle with different particle Reynolds numbers via experimental study, as shown in Fig.5. Based on these experiment data, part of researchers have done considerable research to express the relationship between drag coefficient and particle Reynolds number in empirical formulas with certain particle Reynolds number range, as shown in Table 1.

According to the comparisons of experimental data and predictions of empirical formulas which are presented in Table 2, the method proposed by Turton[12] acquires the minimum relative error which is only 3.06% when compared with experimental data. Therefore, Turton's formula is applied to calculate drag coefficient.

$$C_D = 24(1 + 0.173\,\mathrm{Re}^{0.657}) / \mathrm{Re} + 0.413 / (1 + 16300\,\mathrm{Re}^{-1.09}) \quad \mathrm{Re} < 2 \times 10^5 \tag{15}$$

Table 1 some widely used empirical relationships for estimation of the drag coefficient of sphere particle [11-14]

Empirical relationships	Region of Re	Equation no.
$C_D = \frac{24}{Re}10^E$ $E = 0.261\,Re^{0.369} - 0.105\,Re^{0.431} - \frac{0.124}{1+(\log Re)^2}$	$Re < 3\times10^5$	(5)
$C_D = \frac{24}{Re}\left(1+0.173\,Re^{0.657}\right) + \frac{0.413}{1+16300\,Re^{-1.09}}$	$Re < 2\times10^5$	(6)
$C_D = \left[0.352 + (0.124 + 24/Re)^{1/2}\right]^2$	$0.1 < Re < 10^4$	(7)
$C_D = 1 - 0.5e^{0.182} + 10.11\,Re^{-2/3}\,e^{(0.952\,Re^{-1/4})}$ $-0.03859\,Re^{-4/3}\,e^{(1.3\,Re^{-1/2})} + 0.037\times10^{-4}\,Re\,e^{(-0.125\times10^{-4}\,Re)}$ $-0.116\times10^{-10}\,Re^2\,e^{(-0.444\times10^{-5}\,Re)}$	$0.1 < Re < 10^6$	(8)
$C_D = 24/Re + 6.48\times Re^{-0.573} + 0.36$	$Re < 10^4$	(9)
$C_D = 30/Re + 0.46$	$Re < 10^4$	(10)
$C_D = 24/Re\left(1+0.0654\,Re^{2/3}\right)^{3/2}$	$Re < 10^4$	(11)
$C_D = \left(0.352 + (0.124 + 24/Re)^{1/2}\right)^2$	$Re < 10^4$	(12)
$C_D = \left(0.63 + 4.8\times Re^{-0.5}\right)^2$	$Re < 10^4$	(13)
$C_D = \frac{24}{Re} + \frac{6}{1+Re^{0.5}} + 0.4$		(14)

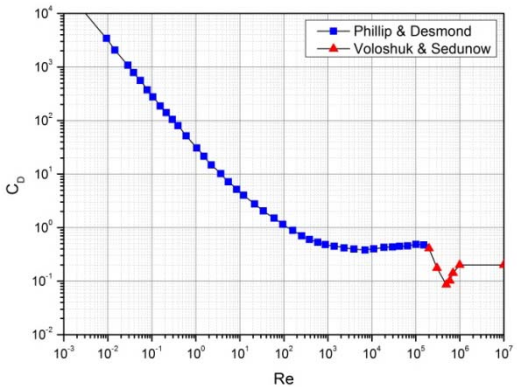

Fig.5 Drag coefficient of rigid sphere particle for the wide range of Particle Reynolds number
Experimental data in this figure are from Ref. [9, 10]

Formulas listed in table 1 and experimental data listed in table 2 are only applicable for the determination of drag coefficient of a single particle without the presence of a neighboring particle. It is necessary to account for the variation of drag coefficient due to the presence of neighboring particles during force calculation of a solid particle on bed surface in inclined pipes. Liang [15] conducted an experiment to study the effect of particles arrangement on the drag coefficient, and the results indicated that the drag force acting on single particle varies significantly with the angular position of neighboring particles. The ratio of drag force acting on particles with the presence of neighboring particles to that acting on a single particle varies from 0.35 to 1.05. Taking all the positions around a bed surface particle into account, an average corrector factor of 0.8 [16] is applied to correct the drag force will be more reasonable. Therefore, the drag force formula applied in this paper is further modified as

$$F_D = 0.8C_D\pi d_p^2\rho_f u^2/8 \tag{16}$$

Table 2 Comparisons of the experimental measuring values of C_D with predictions of equations in table 1 (experimental data are selected from Ref. [9, 10])

Re	Measured C_D	Predicted C_D-values from different equations									
		5	6	7	8	9	10	11	12	13	14
0.01	2502	2447.36	2420.15			2491.05	3000.46	2410.94	2434.74	2364.88	2405.86
0.05	520.37	492.867	491.601			516.423	600.46	486.405	495.674	488.244	485.304
0.1	245.1	245.971	249.147	251.157	204.742	264.602	300.46	245.090	251.157	249.922	244.958
0.5	51.2	49.177	53.266	53.132	49.576	58.000	60.46	50.997	53.132	55.030	51.915
1	27.4	25.835	28.152	27.706	26.452	30.840	30.46	26.392	27.706	29.485	27.400
5	7.3	7.253	7.191	6.610	6.927	7.737	6.46	6.241	6.610	7.710	7.054
10	4.53	4.420	4.285	3.766	4.118	4.492	3.46	3.572	3.766	4.613	4.242
50	1.61	1.542	1.567	1.275	1.466	1.529	1.06	1.245	1.275	1.713	1.623
100	1.08	1.045	1.099	0.913	1.035	1.063	0.76	0.897	0.913	1.232	1.185
500	0.55	0.528	0.562	0.588	0.598	0.592	0.52	0.556	0.588	0.713	0.705
1000	0.462	0.442	0.455	0.543	0.524	0.508	0.49	0.497	0.543	0.611	0.608
5000	0.388	0.393	0.393	0.505	0.456	0.414	0.466	0.433	0.505	0.487	0.488
10000	0.408	0.418	0.420	0.501	0.456	0.395	0.463	0.421	0.501	0.460	0.462
50000	0.466	0.491	0.470		0.484						0.427
100000	0.483	0.434	0.471		0.437						0.419
Relative error(%)		3.71	3.06	13.39	8.86	5.83	17.78	8.7	11.9	12.07	10.18

The lift forces on cuttings are caused either by fluid velocity gradient or cuttings rotation. The Magnus force is the list force generated by a pressure differential between both sides of cuttings resulting from the velocity differential due to the cuttings rotation. As the rotation of the cuttings is mostly caused by the fluid flow, the rotation speed is close to the local rotation of fluid. According to the study of Crowe et al [17], the Magnus force is close to 0 and can be neglected.

Fluid shear can exert a lift force on the cuttings in solid-liquid two phase flow, which is known as Saffman force and the force is in the direction perpendicular to the relative velocity between the cuttings and fluid. Saffman[18]first found that particle would experience the lift force during transportation in viscous fluid. On the basis of assumptions of unbounded linear shear flow and constant velocity gradient, Saffman derived a formula to estimate the lift force via Navier-Stokes equation:

$$F_L = 6.46\rho_f u d_p^{\ 2}\left(\eta du/dy\right)^{1/2} \tag{17}$$

However, as Saffman only accounting for the component of the particle velocity paralleled to the mean flow, the correlation is only valid for cuttings transportation in no-boundary fluid flow and cannot be used for cuttings on or near a surface. On the analogy of the drag force calculation method, Clark & Bickman [4] proposed that the lift force correlation could be expressed as

$$F_L = C_L \pi d_p^2 \rho_f u^2 / 8 \tag{18}$$

And they introduced lift coefficient for the cuttings resting on the sedimentary bed. The lift coefficient is given as follows:

$$C_L = 0.178 \tag{19}$$

Or

$$C_L = 5.82\left(\alpha_p / Re_p\right)^{1/2} \tag{20}$$

Where $\alpha_p = d_p / 2u \cdot \left|du/dr\right|$

Through cuttings transportation experiments, researchers have found that rolling transport existed during bed surface cuttings transportation in inclined pipes. Especially at high inclination angle, cuttings will roll and bounce along the bed surface. As shown in Fig.4, assuming that the surface particle is on the threshold of rolling around the contact point and neglecting the friction force between cuttings, the dynamic torque acting on the particle is equal to the static torque, thus:

$$F_D d_p \sin\phi/2 + F_L d_p \cos\phi/2 = F_W d_p \sin(\phi+\alpha)/2 \quad (21)$$

Substituting equations (1) (16) and (18) into equation (21) we will obtain the minimum rolling transport velocity:

$$u_r = \left[\frac{4d_p g(s-1)\sin(\phi+\alpha)}{3(0.8C_D \sin\phi + C_L \cos\phi)}\right]^{0.5} \quad (22)$$

Where $s = \rho_p / \rho_f$

When the fluid flow rate increases to a certain value, cuttings on bed surface will be suspended and get into suspension transport. As shown in Fig.4, assuming a surface particle is on the threshold of suspension, and then the balance of forces in the X-Y directions can separately be expressed as:

$$F_D = F_W \cos\alpha \quad (23)$$

$$F_L = F_W \sin\alpha \quad (24)$$

Substituting equations (1) (3) and (18) into equation (23) and (24), we will obtain the minimum suspension transport velocity in X-Y directions respectively:

$$u_{susx} = \left[4d_p g(s-1)\cos\alpha/(3C_D)\right]^{0.5} \quad (25)$$

$$u_{susy} = \left[4d_p g(s-1)\sin\alpha/(3C_L)\right]^{0.5} \quad (26)$$

Analyzing equations (15) and (16) we can obtain:

$$u_{susy}/u_{susx} = \left[\tan\alpha C_D / C_L\right]^{0.5} \quad (27)$$

EXPERIMENT

In this experiment, two sphere cuttings with diameter of 3, 5mm and of density 2700kg/m^3 have been used. In order to minimize the end effects in the test section, a smooth plexiglass pipe with internal diameter of 50 mm and length of 4000 mm was used. And two types of Newtonian fluids, namely, water and glycerol solution of density 1000, 1150 kg/m3 and of viscosity 0.001, 0.01 Pa•s at 20℃ were used as the test fluid. Table 3 lists all physical properties of cuttings and fluids used in experiment and mathematical calculation.

Table 3 Physical properties of test cuttings and fluids

Cuttings diameter (mm)	3, 5	
Cuttings density (kg/m^3)	2700	
Fluid density (kg/m^3)	Water	1000
	Glycerol solution	1150
Fluid viscosity (Pa・s)	Water	0.001
	Glycerol solution	0.01

A frame was fabricated in which the plexiglass pipe could be fixed and the frame could be fixed at any inclination from horizontal to vertical. A universal bevel protractor fixed on the frame was used to measure the inclination angle. In this work, the angle of inclination varied from 0° to 90° with a difference value of 10° .

The fluid and the cuttings were loaded into the circulate system and left at least 24h prior the experiment for thermal equilibrium to be reached and for the trapped air bubbles to escape. The test section was located in the middle of the pipe and was sufficiently away from the entrance and top end for minimizing the end effects and allowing the constant velocity to be attained [19].The fluid velocity was measured by the flowmeter.

At the beginning of the experiment, turned the pump on and circulated the fluid at a low displacement and kept the cuttings on bed surface remaining stationary. After the system coming to stable state, increased the pump

displacement gradually and observed the motion of sphere cuttings on bed surface. Recorded the flowmeter reading when the cuttings began to move. Then adjusted the inclination angle of pipe and repeated the experiment process.

RESULTS AND DISCUSSION

For cuttings suspension transport, it is interesting to analyze equations (25) and (26) when the inclination angle varies from vertical to horizontal. Apparently, equation (25) calculated the minimum fluid velocity for cuttings coming into force balance in the X-axis direction varies with the angle inclination and equation (26) calculated the minimum fluid velocity for cuttings coming into force balance in the Y-axis direction varies with the angle inclination. As shown in Fig. 6, the Y-axis minimum suspension velocity of cuttings wakens as the inclination angle increases and simultaneously, X-axis minimum suspension velocity gradually reduces. Furthermore, the pattern of critical suspension velocity in X-Y axis that shown in Fig. 6 obviously indicates that there is a point of intersection at low inclination angle. Based on equation (27), the position of intersection point of X-Y axis minimum suspension velocity curves depends on drag coefficient, lift coefficient and the inclination angle. Therefore, the cuttings come to a critical state of suspension only with the values of X-Y axis minimum suspension velocity beyond the intersection point.

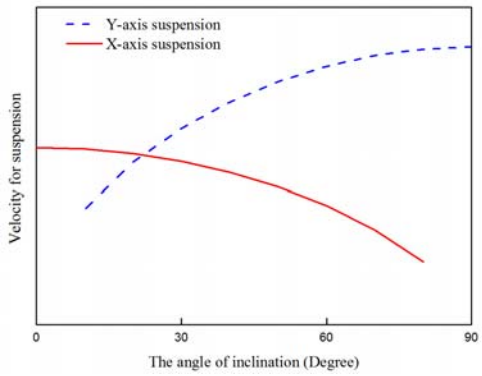

Fig.6 Pattern of critical suspension velocity of cuttings in X-Y axis in an inclined (uphill transport) pipe

Then for cuttings critical incipient velocity, it is interesting to analyze equations (22), (25), (26) and (27) when the inclination angle varies from vertical to horizontal, as shown in Fig. 7. The figure shows the effect of inclination angle on critical suspension velocity and critical rolling velocity. Furthermore, the critical velocity curves in Fig. 7 obviously indicates that one cuttings transport mechanism takes precedence over the other at a situation with a given inclination angle. The suspension transport mechanism dominates cuttings transportation at low inclination angle (usually less than 30°), while rolling transport mechanism dominates cuttings transportation in the range of medium angle to horizontal and both of them coincide with the cuttings transport mechanism analyzed in section 2. We should notice that it is theoretical to assume a single mechanism dominate cuttings transportation in a certain time, but suspension and rolling mechanism may simultaneously appear in practice due to the complication of liquid-solid flow.

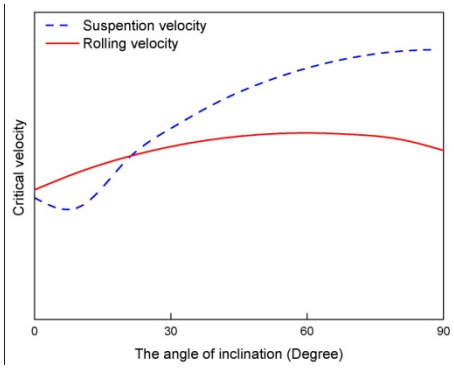

Fig.7 Pattern of critical velocity of cuttings rolling and suspension transport in an inclined (uphill transport) pipe

Table 4 presents experimental results of critical incipient velocity tests of water and glycerol solution. For identical condition, the experimental data were measured repeatedly to check the reproducibility and the average value of measurement results was recorded in table 4. Predictions of the model under water and glycerol solution test

conditions are also presented in Table 4. Apparently, the measurement results are smaller than model predictions in general. This phenomenon is likely due to the turbulence of flow which will cause the reduction of critical incipient velocity has not been taken into account in the model. However, the predictions show satisfactory agreement with the measurement results as shown in Fig.8 and Fig.9. The mean relative error is 3.66% (water, particle diameter 3mm), 3.26% (water, particle diameter 5mm), 4.44% (glycerol solution, particle diameter 3mm) and 4.72% (glycerol solution, particle diameter 3mm) respectively.

Table 4 A comparison of the experimentally determined critical incipient velocity with the model predictions

Inclination angle (degree)	Experimental data of critical incipient velocity (m/s)				Model predictions of critical incipient velocity (m/s)			
	Water		Glycerol solution		Water		Glycerol solution	
	dp=3mm	dp=5mm	dp=3mm	dp=5mm	dp=3mm	dp=5mm	dp=3mm	dp=5mm
0	0.376	0.518	0.216	0.323	0.3900	0.5340	0.1999	0.3169
10	0.362	0.496	0.207	0.304	0.3870	0.5298	0.1983	0.2931
20	0.353	0.485	0.261	0.402	0.3767	0.5072	0.2751	0.4114
30	0.420	0.571	0.288	0.434	0.4405	0.5873	0.2950	0.4500
40	0.447	0.593	0.297	0.44	0.459	0.6108	0.3090	0.4698
50	0.456	0.632	0.308	0.486	0.4701	0.6247	0.3173	0.4816
60	0.473	0.647	0.319	0.492	0.4800	0.632	0.3231	0.4856
70	0.462	0.605	0.304	0.475	0.4701	0.6247	0.3173	0.4816
80	0.446	0.594	0.288	0.454	0.459	0.6108	0.3090	0.4698
90	0.430	0.572	0.310	0.432	0.4405	0.5873	0.2950	0.4400
mean relative error (%)					3.66	3.26	4.44	4.72

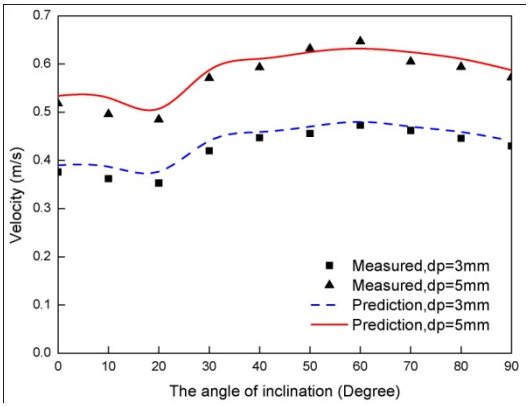

F

ig.8 Comparison between the experimental values and model predictions of critical incipient velocity of different particles as a function of inclination angle using water

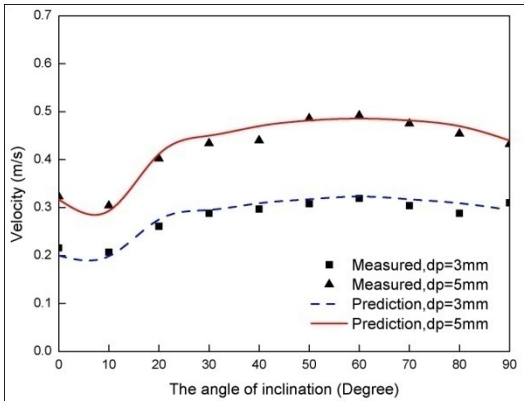

Fig.9 Comparison between the experimental values and model predictions of critical incipient velocity of different particles as a function of inclination angle using glycerol solution

Model predictions and measurement results of critical incipient velocity as a function of inclination angle using water and glycerol solution are separately presented in Fig. 8 and Fig. 9. The results indicate that the cuttings size, inclination angle and fluid properties significantly affect the critical incipient velocity. Furthermore, the results also confirm the pattern of critical incipient velocity curves of cuttings rolling and suspension transport in Fig.7. And the critical incipient velocity comes to the maximum value at about 60° of inclination and comes to the minimum value at low inclination angle. Furthermore, according to equations (25), (26) and (27), the minimum value position

depends on drag coefficient, lift coefficient and inclination angle.

CONCLUSION

There are two main transport mechanisms for cuttings transport in inclined pipes:(i) suspension transport mechanism takes precedence at low inclination angle; (ii) in the range of medium angle to horizontal, rolling transport mechanism dominates cuttings transport when fluid velocity is low while suspension transport mechanism gradually comes to domination as the increase of fluid velocity. Drag coefficient calculation method is optimized to improve the prediction accuracy of simplified mechanistic model and Turton's method was proven to obtain the minimum relative error which was only 3.06% compared with experimental data. Predictions of the simplified mechanistic model which presented in this paper are in good agreement with the measured experimental data and the relative error is less than 5%. Model predictions and experiment measurements indicate that the critical incipient velocity reaches the maximum value at about 60° of inclination and comes to the minimum value at low inclination angle. And the position of minimum value is determined by drag coefficient, lift coefficient and inclination angle.

Acknowledgments
The authors gratefully acknowledge for the financial support by The National Basic Research Program of China(No. 2010CB226704) and Science Foundation of China University of Petroleum ,Beijing (No. 2462013BJRC002)

REFERENCES

[1] SubhasishDey.*Applied Mathematical Modeling*, v 23, n5,p 399-417,**1999**.
[2] G. Ziskind, M. Fichman, C. Gutfinger. *Journal of Aerosol Science*, v 26, n 4, p 613-644, **1995**.
[3] J.T. Ford, ErhuGao, M.B. Oyeneyin. *SPE Drilling & Completion*, v 11, n 3,p 168-172, **1996**.
[4] R.K. Clark,K.L.Bickham.*SPE Annual Technical Conference and Exhibition*,**1994**.
[5] A Ramadan, P Skalle, S.T Johansen.*Chemical Engineering Science*, v 58,p 2153-2163,**2003**.
[6] Y. Tsuji, N. Kato, T. Tanaka. *International Journal of Multiphase Flow*, v 17, n3,p343-354, **1991**.
[7] P.J.C. Caulet, R.G.J.M. van der Lans, K.Ch.A.M. Luyben.*The Chemical Engineering Journal and the Biochemical Engineering Journal*, v 62, n 3,p 193-206,**1996**.
[8] H Meng, CWM Van Der Geld. *Liquid Solid Flows, ASME*, v 118,p183–190, **1991**.
[9] Phillip P. Brown. *Journal of Environmental Engineering-ASCE*, v 129, n 3,p 222–231, Mar **2003**.
[10]V.M. Voloshuk, J.S. Sedunow.The processes of coagulation in dispersedsystems. Nauka, Moscow, **1971**.
[11] R.L.C. Flemmer, C.L. Banks.*PowderTechnology*, v 48, n3,p217–221,**1986**.
[12] R. Turton, O. Levenspiel.*Powder Technology*, v 47, n 1, p83-86,**1986**.
[13] R.P. Hesketh, A.W. Etchells, T.W.F. Russell.*Chemical Engineering Science*, v 46, n 1, p 1-9, **1991**.
[14]KadimCeylan, Ayşe Altunbaş. *Powder Technology*,v 19, n2–3,p 250-256,**2001**.
[15]S.-C. Liang, T. Hong.*International Journal of Multiphase Flow*, v 22, n 2, p 285-306, **1996**.
[16]MingqinDuan, Stefan Miska.*SPE Drilling & Completion*, v 24, n 2, p 229-238, **2009**.
[17] CT Crowe, JD Schwarzkopf. Multiphase flows with droplets and particles. CRC Press, Boca Raton, FL, p471, **1998**.
[18] PG Saffman. *Journal of Fluid Mechanics*, v 22, n 2,p 385-400,**1965**.
[19] R.P. Chhabra, J.M. Ferreira.*Powder Technology*, v 104, n 2, p 130-138, **1999**.